ELSEVIER

Contents lists available at SciVerse ScienceDirect

Organic Electronics

journal homepage: www.elsevier.com/locate/orgel



Second-order distributed feedback polymer laser based on holographic polymer dispersed liquid crystal grating



Wenbin Huang ^{a,b}, Yonggang Liu ^a, Lifa Hu ^a, Quanquan Mu ^a, Zenghui Peng ^a, Chengliang Yang ^a, Li Xuan ^{a,*}

^a State Key Laboratory of Applied Optics, Changchun Institute of Optics, Fine Mechanics and Physics, Chinese Academy of Sciences, Changchun 130033, China ^b Graduate School of Chinese Academy of Sciences, Beijing 100039, China

ARTICLE INFO

Article history: Received 3 March 2013 Received in revised form 3 May 2013 Accepted 20 May 2013 Available online 3 June 2013

Keywords:
Distributed feedback organic laser
Semiconducting polymer
Nanostructure fabrication
Holographic polymer dispersed liquid
crystal

ABSTRACT

We report on the fabrication and characterization of a second-order distributed feedback (DFB) polymer laser based on a holographic polymer dispersed liquid crystal (HPDLC) transmission grating. The fine organic grating is fabricated on top of the homogeneous conjugated polymer layer in a one-step process. The device shows surface-emitting, single mode laser emission with a threshold of $13.3~\mu J/cm^2$, and the working characteristics merely degrade after 10 months of storage in ambient atmosphere. We further explain the dependence of threshold on pumping length, and demonstrate the small refractive index modulation of this all-organic grating is sufficient to maintain efficient DFB laser action. This simple working structure, combined with large processing area provided by the holographic polymerization technique, is extremely promising in realizing ultra-low cost plastic lasers.

© 2013 Published by Elsevier B.V.

1. Introduction

Organic semiconductor lasers (OSLs) have attracted a broad scientific interest since the first demonstration of stimulated emission in semiconducting polymer in 1992 [1]. Thanks to the salient features of organic materials, OSLs are cost effective, tunable across the whole visible spectrum and mechanically flexible [2,3]. Due to some additional loss mechanisms under electrical injection [4,5], there has been no demonstration of organic laser diodes. Fortunately, indirect electrical pumping with cheap inorganic diode lasers [6] or light emitting diodes [7] is possible as OSLs exhibit very low operational thresholds. Distributed feedback (DFB) resonator configuration has attracted the most attention in OSLs [3], because it exhibits several advantages, such as compatibility with processing technique of organic thin film, no need of cleaved edge for output, excellent mode selection and low working threshold. In publications about organic DFB lasers, two kinds of configurations are commonly used: the active medium is over-coated onto the corrugated substrate [8] or the grating structure is directly written into the active layer [9]. In either case, the thickness of active layer is strongly modulated, and the grating depth in the active layer has been demonstrated as a complex parameter to be optimized [10]: (1) The DFB coupling mechanism is complex and uncertain, as the corrugations in the active layer provide both gain and index modulation. In some cases, the feedback is attributed to gain coupling because the lasing peak locates at the dip of band gap [8]. While in some cases, the feedback is attributed to index coupling as the lasing peak locates at the long wavelength edge of the band gap [11]. This uncertainty brought by grating depth in the active layer rends laser threshold reduction through optimizing coupling coefficient difficult. (2) The effective thickness and refractive index of the waveguide core layer which are essential to estimate the location of lasing wavelength and number of lasing modes are uncertain. They are inevitably modulated by the amount of other

^{*} Corresponding author. Tel.: +86 13756288515. E-mail address: xuanli@ciomp.ac.cn (L. Xuan).

materials filling in the corrugations, which in turn are affected by the grating depth in the active medium. The significance of this effect varies from device to device, and is extremely pronounced when the grating depth is comparable to the active medium thickness.

In addition to the working structure, there is still potential in developing new techniques for fabricating the periodic microstructures used in organic lasers. Electron beam lithography in combination with dry etching techniques [12,13] give very sharp edged gratings with narrow periods, but it requires sophisticated experimental equipment and a sequence of fabricating steps. These techniques are not compatible with the initial motivation of easy processing of organic materials. As for the various methods in nanoimprint lithography, hot embossing will bring deleterious effect to fluorescence property of the gain medium [14,15], and liquid imprinting [9] or solvent-assisted [16] techniques cannot give high quality gratings. The UV nanoimprint lithography [17] may be the most promising, but it does not provide an easy way to alter the grating period. Additionally, the laser ablation technique [18,19] requires a careful selection of the gain medium.

In our pervious publication [20], we report on the first fabrication of third-order DFB polymer lasers based on holographic polymer dispersed liquid crystal gratings. The organic grating is fabricated separately on top of the homogeneous conjugated polymer layer. This technique is a variation of the holographic polymerization, and has the advantages of large processing area, low cost, easiness to vary the grating period. It also does not bring any deleterious effect to the gain medium and can be applied to any kind of active medium, as the fabrication requires no harsh conditions. Moreover, the working characteristics are good, with a threshold of $21 \,\mu\text{J/cm}^2$ and a bandwidth of 0.7 nm. In this paper, we report on the fabrication and characterization of a second-order DFB polymer laser using a small period HPDLC grating. In addition to all the advantages of the third-order one, this polymer laser shows surfaceemitting laser emission with a threshold of 13.3 μ J/cm². We further give explanations on the threshold dependence on pumping length, and find the comparatively low refractive index modulation afforded by this organic grating is sufficient to maintain efficient optical feedback. Besides, the laser performances of these devices merely degrade after 10 months of storage in ambient atmosphere, indicating the stability of the organic grating in providing feedback. Thus, we think this "organic" approach is extremely compatible with organic semiconductors, and can provide ultra-low cost plastic lasers.

2. Device fabrication

Conjugated polymer Poly(2-methoxy-5-(2'-ethyl-hexyloxy)-p-phenyl-enevinylene) (MEH-PPV) (Average molecular weight $\sim\!120,\!000;$ photoluminescence quantum yield $\sim\!10\%)$ was purchased from Jilin OLED Material Corporation and used as received. The solution of MEH-PPV in xylene (6 mg/ml) was deposited onto a glass substrate by spin-coating (1700 rpm), resulting in a homogeneous thin film of MEH-PPV with a thickness of $\sim\!80\,\mathrm{nm}$

measured by a Dektak Profilometer. The thickness here is chosen as the optimized value, which enables sufficient evanescent wave spread into the grating layer for feedback [20]. Then an empty cell was made with another uncoated glass substrate, where the cell gap was controlled as $\sim 6~\mu m$ by Mylar spacers. After that, the prepolymer syrup containing monomers, liquid crystal (LC) and photo-initiator was injected into the cell via capillary effect in the dark. For a direct comprehension of above processes or detailed chemical composition of the mixture, readers may refer to [20].

The writing setup for HPDLC grating is shown schematically in Fig. 1. A frequency-doubled, continuous wave Nd-YAG laser at λ_w of 532 nm is used as the writing light source. After filtered and collimated by the beam expander, the laser beam is divided into two beams with equal intensity. The two beams are then directed by two mirrors and recombine at the cell surface with an intersecting angle of θ . The grating period Λ can be calculated and precisely controlled according to $\Lambda = \frac{\lambda_W}{2 \sin \theta / 2}$. The DFB lasing wave- λ_{las} should obey the Bragg equation $\lambda_{las} = 2n_{eff} \Lambda/m$, where n_{eff} is the effective refractive index of the laser mode and m is the Bragg order. n_{eff} mainly depends on the thickness of MEH-PPV layer and refractive indices of three different layers, which is calculated as \sim 1.60 previously by us [20]. Considering the gain spectrum of MEH-PPV is around 630 nm [11], the grating periodicity for the third-order laser and second-order one should be selected as 596 nm (corresponding to an intersection angle of 53°) and 394 nm (corresponding to an intersecting angle of 85°), respectively. During the holographic exposure process, monomers would polymerize preferentially in bright fringes, causing a chemical potential gradient both in monomer and LC across the fringe patterns. Then monomers would diffuse to bright regions to continue photo-polymerization, and the unreacted LC would diffuse to dark regions. At some point, the chemical miscibility between monomer and LC breaks, leading to the phase separation of LC. For efficient LC phase separation, the choice of curing intensity is very important. The optimal curing condition for the narrower grating is different due to two reasons: first, an increase in the intersecting angle would bring an increase in the effective exposure area in the sample, resulting in decreased exposure

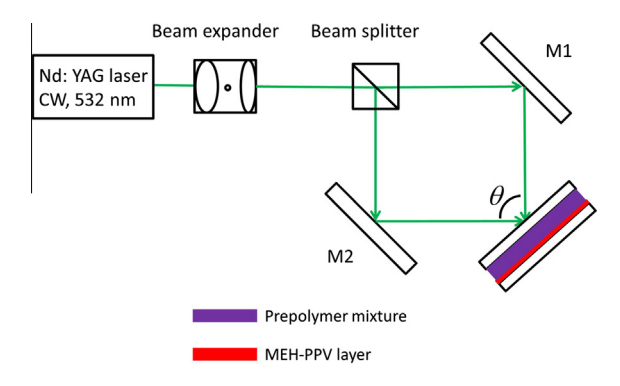


Fig. 1. Schematic experimental setup for the fabrication of HPDLC gratings.

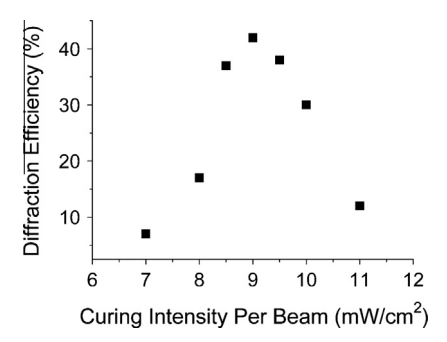


Fig. 2. Diffraction efficiency of second-order HPDLC grating as a function of curing intensity.

intensity; second, the narrower grating pitch would influence the diffusion dynamics of monomer and LC during the grating formation. Thus we varied the curing intensity gradually to study the grating performance. The diffractive properties of resulted gratings were characterized with a He-Ne laser (1 mW; 632.8 nm), placed at the first Bragg angle. The diffraction efficiency was determined as $\eta = I_1/I_1$ $(I_0 + I_1)$, where I_0 and I_1 are the intensity of zeroth diffraction order (transmitted beam) and first diffraction order, respectively. The result is shown in Fig. 2, and a curing intensity of 9 mW/cm² gives best gratings. The highest diffraction efficiency is about 45%, while a value of 90% can be obtained in gratings with a period larger than 1 µm [21]. This is due to the decreased LC phase separation with the decrease in grating period, and there exists a cut-off value $(\sim 0.4 \lambda_w)$ of fringe spacing below which no HPDLC gratings can be formed [22]. The mild HPDLC grating formation conditions (9 mW/cm², 40 s) here could not bring any deleterious effect to the fluorescence property of the conjugated polymer, as the pumping intensity during the lasing measurement is always over 1 kW/cm².

3. Sample characterization

Fig. 3a is an image of the resulted device when the sample is placed flat. As the organic grating layer is transparent and shows little scattering, the sample exhibits the homogeneous MEH-PPV layer. Fig. 3b is an image of the sample when it is tilted. Due to the diffractive property of the grating, the region covered by organic grating is¹ colorful. The size of grating region is about $2\,\text{cm}\times2\,\text{cm}$, covering almost the whole cell. For a more detailed characterization of the device structure, the cross section of the sample was analyzed through scanning electron microscope (SEM). For the test, the cell was opened and the two glass substrates were separated by hand. Then the substrate with both MEH-PPV layer and organic grating layer was immersed in ethanol for several hours to remove the LC. During this process, the two layers could detach from the glass substrate. Then the film was mounted on the testing board and over-coated with a thin film of gold nanoparticles to improve the conductivity. Fig. 3c is a low-voltage SEM image showing the cross section of the whole film, where the holes are regions previously occupied by LC. The thin active layer is difficult to be distinguished from the grating layer in Fig. 3c. What we do care here is the depth of the corrugations in the grating layer, which penetrates through the 6 µm cell. In this three layered structure, the feedback which is essential to laser action is obtained by the interaction between the grating layer and the evanescent wave spread from the active layer [20]. As the penetration depth of evanescent wave is very short (\sim 0.5 µm), there much be corrugations lying close to the active layer for efficient feedback. This requirement can be easily fulfilled in our device due to the deep corrugations. Fig. 3d shows the cross section of the film at high magnification. The active layer is neither dissolved by the prepolymer mixture, nor destroyed during grating formation. Thus, the active layer and grating layer can be characterized separately, which is an advantage of this working structure. The conjugated polymer also adheres tightly to the organic grating layer, and can be protected from oxygen and moisture during lasing measurement.

4. Device performance

The lasing property of the resulted device was investigated under ambient atmosphere using a frequency-doubled, pulsed Nd-YAG laser (532 nm, 8 ns, 1 Hz). The schematic setup is shown in Fig. 4. After being expanded and collimated, the pump beam was shaped by a cylindrical lens into a strip. The sample was placed approximately at the focal point of the cylindrical lens and the normal of cell was tilted $\sim 20^{\circ}$ with respect to the incident pump beam. The width of the pumping strip at the sample was about 100 μm. The length of the pumping strip was controlled by an adjustable slit, and only the central part (less than 0.3 cm) of the beam was selected to ensure the uniformity of the pumping strip. For a real-time detection of pump energy, a beam splitter was placed between the slit and sample and one of the split beams was directed into an energy meter. The vertical output emission from the sample was measured using a fiber coupled spectrometer with a resolution of 0.3 nm.

4.1. Lasing properties

When the pump energy is above laser threshold, the device emits a bidirectional emission along the normal of the cell. The inset in Fig. 5 shows the lasing beam pattern on the paper screen. It consists of two tangent arc lines, which is typical in the performance of one-dimensional second-order DFB lasers [3]. Fig. 5 also shows the spectrum of the vertical emission at a pump energy of $2.5\times$ threshold. The single sharp peak with a bandwidth of 0.6 nm locates at 628.5 nm, and there is no background of amplified spontaneous emission (ASE). ASE is well suppressed by the mode supported by the organic cavity, and energy can be effectively channeled into laser emission. The feedback mechanism here is attributed to pure index coupling, as the active layer is homogeneous and gain modulation is not present in this device. This coupling

 $^{^{\}rm 1}$ For interpretation of color in Fig. 3, the reader is referred to the web version of this article.

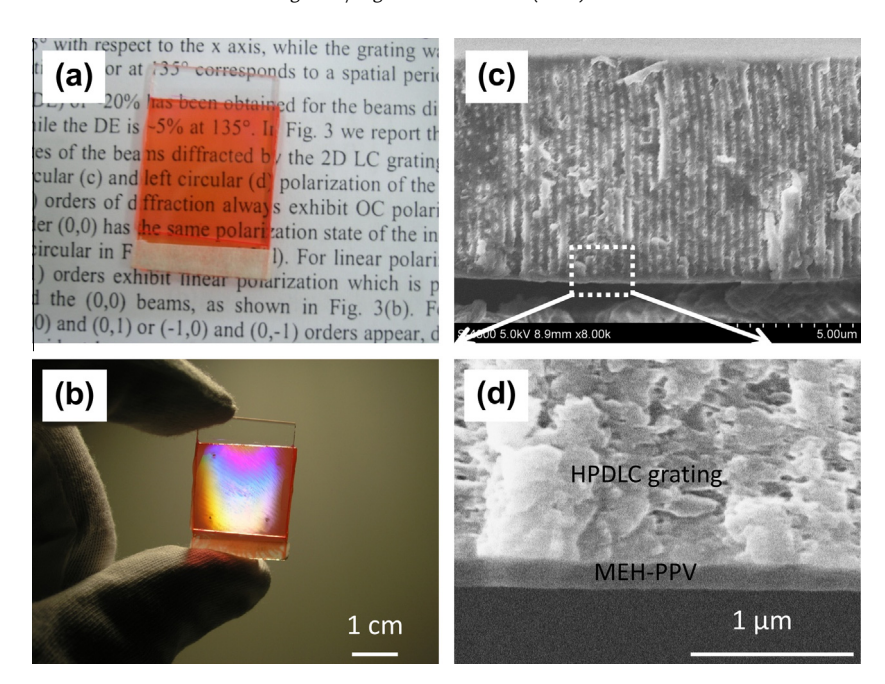


Fig. 3. (a) Photograph of the sample when it is placed flat. (b) Photograph of the sample when it is tilted. (c) SEM picture of the film cross section. (d) Zoomed SEM picture of the side view.

mechanism can support two lasing modes situated below and above the band gap [11]. Fortunately, the radiation loss in second-order laser cavity provides an additional mode selection mechanism [23], and only one lasing peak can be found. Fig. 6 shows the dependence of output energy on input energy, where the length of the pumping strip was controlled as 0.3 cm. The threshold is indicated by a sudden increase in the slope, which is about 13.3 μ J/ cm² (corresponding to 1.66 kW/cm²). It is a common value in literature, but the fabrication of our device is much easier. In addition to the difference in the number of output lasing beams, the second-order laser shows a 40% reduction in threshold when compared with the third-order one. Thus, second-order DFB laser is more promising in actual use. This result further confirms the ability of HPDLC technique in providing narrow gratings for second-order DFB lasers.

4.2. Dependence of threshold on pumping length

There are implications in other publications [24] that a high refractive index modulation could result in a high performance laser device due to the increased coupling coefficient. While the small refractive index difference between organic materials is a natural property, question may arise concerning whether it could be a bottleneck in using HPDLC gratings as organic laser cavities. Here, through the explanations on the dependence of threshold on pumping length, we demonstrate that the refractive index modulation afforded by HPDLC gratings is sufficient for efficient feedback as long as the pumping region is longer than 0.03 cm.

Although the prepolymer syrup is exposed to a sinusoidal intensity profile, the resulted sample shows

a nonsinusoidal grating profile with higher order harmonics. In this case, the refractive index along the grating vector can be expressed as [25]:

$$n(x) = n_0 + n_1 \cos\left(\frac{2\pi}{\Lambda}x\right) + n_2 \cos\left(\frac{4\pi}{\Lambda}x\right) + \cdots \tag{1}$$

where Λ is the grating spacing, n_0 is the average refractive index of the grating, and n_1 and n_2 are refractive index modulations at the basic and doubled spatial frequencies. n_1 and n_2 are responsible for the first- and second-order physical processes, respectively. It is known that, in second-order DFB lasers, the laser emission is coupled out of the waveguide through a first-order effect and the counter propagating waves are coupled together through a secondorder effect [11]. An easy and direct way to obtain refractive index modulation at each order is by measuring the diffraction efficiencies at several Bragg angles [25]. Due to the small grating period, the initial attempt to measure the diffraction efficiency at second Bragg angle of the grating was unsuccessful. In order to get a reasonably precise value for n_2 , we measured the diffraction efficiencies at different Bragg angles of a set of gratings with a large period of \sim 800 nm, and found the nonlinearity $\frac{n_1}{n_2}$ of HPDLC gratings is around 3. Finally, we estimated a value of 6×10^{-3} for n_2 , and it is responsible for the optical feedback in our second-order DFB laser. It is worth to mention here that the diffraction efficiency measurements are all with an s-polarized He-Ne laser, as the output lasing is totally TE polarized.

We found the threshold condition for pure index coupling by Kogelnik and Shank [26] could be used to explain the threshold performance of this DFB laser. The device fulfills the requirements of the theoretical work in below aspects: first, the pumping scheme falls in the quasi-steady

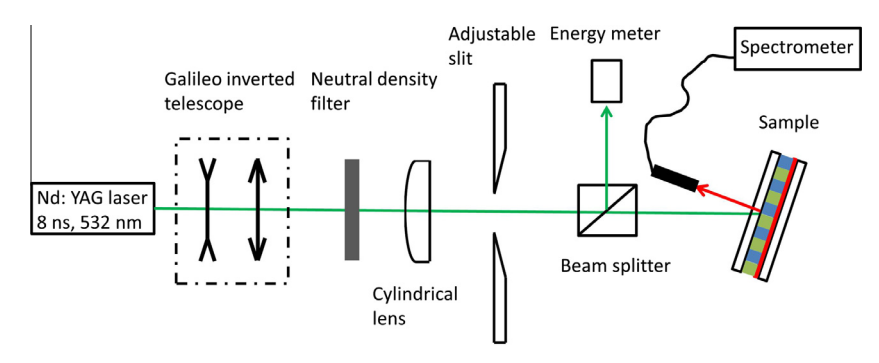


Fig. 4. Schematic setup for the optical pumping of the sample.

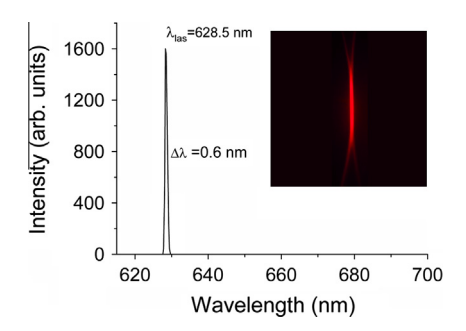


Fig. 5. Output lasing spectrum at $2.5 \times$ threshold. The inset shows the vertical laser emission on a paper screen.

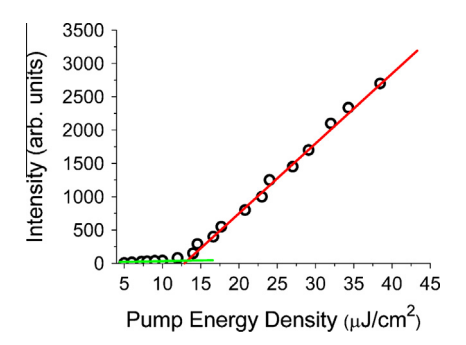


Fig. 6. Output energy as a function of pump energy density, indicating a pump threshold of about 13.3 $\mu J/cm^2$.

regime, as the duration of the pumping pulse (8 ns) is much longer than lifetime of singlet excited states (\sim 1 ns). Second, gain modulation is not present in the homogeneous active layer, and the feedback mechanism is attributed to pure index modulation. Further, according to the criterion for the strength of the coupling coefficient $\left(\frac{\lambda_{in}}{\log L}\right)^2$, which is less than 0.5 when the pumping length L is longer than 0.02 cm, indicating the working of the studied DFB devices falls in high coupling strength (low-gain) regime. Thus the threshold condition is:

$$\alpha_{thres}L \approx \left(\frac{\lambda_{las}}{n_2L}\right)^2$$
 (2)

where α_{thres} is the net gain coefficient at threshold, which is the difference between optical gain and loss:

$$\alpha_{thres} = \sigma N_{thres} - \alpha_{loss} \tag{3}$$

As the simulated cross section σ is a constant and the threshold inversion population density N_{thres} is in proportion to threshold pump energy density [3] (do not reach the regime of saturation). Eq. (3) can be rewritten as:

$$\alpha_{thres} = GI_{thres} - \alpha_{loss} \tag{4}$$

where I_{thres} is the threshold intensity, G is slope for gain coefficient in cm/W, and α_{loss} is the loss coefficient including scattering, output radiation and reabsorption which is independent of the pumping length. G is a very important parameter characterizing the effectiveness of the laser device, and it mainly depends on the gain medium and working structure. We measured the gain coefficient slop G via the variable strip length method (See Appendix A. Supplementary material). The obtained G is around 0.016 cm/W, which is comparable to that in [27]. Eq. (2) can be rewritten in below form:

$$I_{thres}(L) = \frac{1}{G}\alpha_{loss} + \frac{1}{G}\left(\frac{\lambda_{las}}{n_2}\right)^2 \frac{1}{L^3} \tag{5}$$

Considering $I_{thres}(0.3~\text{cm}) \approx I_{thres}(\infty) = \frac{1}{G}\alpha_{loss}$, Eq. (5) can be further written as:

$$I_{thres}(L) = I_{thres}(0.3 \text{ cm}) + \frac{1}{G} \left(\frac{\lambda_{las}}{n_2}\right)^2 \frac{1}{L^3}$$
 (6)

The dependence of laser threshold on pumping length predicted by Eq. (6) is shown in Fig. 7, where the open squares are experimental data. The curve predicts a critical length below which the laser threshold increases significantly, and it has been experimentally observed by Calzado et al. [28] recently. The precise measurements of the threshold with a pumping length less than 0.03 cm were not performed here, limited by the sensitivity of our detector. What we care more in this work is that, the laser threshold merely increases when the pumping length is decreased to 0.03 cm. The reason for this lies in the last term in Eq. (5). As the refractive index modulation n_2 (6×10^{-3}) of HPDLC grating is comparatively large, a decrease of the pumping length L down to 0.03 cm would only bring an increase of 250 W/cm² in threshold. This increase in threshold can be negligible (only about one tenth of the threshold at 0.3 cm pumping length) during actual measurements. These experimental results and theoretical explanations show the comparatively low refractive index

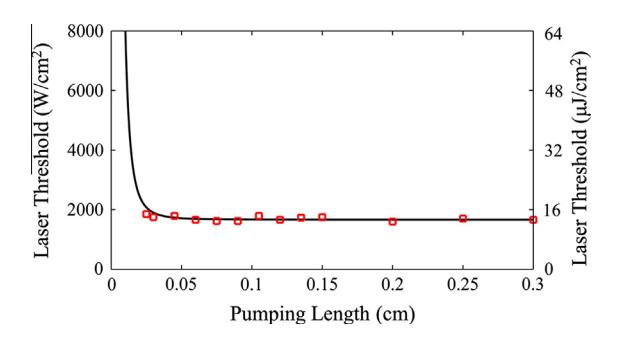


Fig. 7. Dependence of laser threshold on pumping length predicted by Eq. (6). Open squares are experimental data.

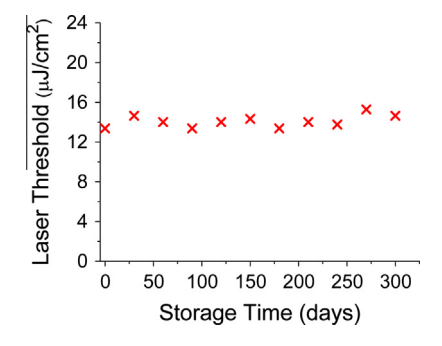


Fig. 8. Dependence of laser threshold on storage time.

modulation afforded by HPDLC gratings works equally well as a high refractive index modulation for providing feedback as long as the pumping length is longer than 0.03 cm.

In most publications, a pumping spot is often used instead of a strip. We changed the cylindrical lens into a spherical lens, and diameter of the pumping spot on the sample was ~0.05 cm. The threshold under the spot pumping is ~1700 W/cm², almost the same as the strip pumping. In fact, the pumping spot could be regarded as a sequence of pumping strips with different lengths, and the measured threshold is determined by the longest strip (equal to spot diameter). The top and bottom caps of the spot with a length shorter than 0.03 cm cannot reach the threshold, and would lead to a decrease in output lasing intensity. Some simple calculations show the region covered by the two caps are less than one tenth of the total spot area (for spot diameter larger than 0.05 cm), and would have little influence on laser performance.

4.3. Stability of HPDLC grating in providing feedback

Working lifetime is a crucial aspect of organic lasers. Encapsulation is often required to improve the operational lifetime, as the organic emitters are susceptible to photo-induced oxidation which can degrade the fluorescence property [29]. In our device, the organic HPDLC grating layer could insulate the MEH-PPV layer from oxygen and moisture naturally. The lifetime of the organic laser is ultimately limited by photoinduced cross-linking of the gain medium [30]. In addition to the lifetime of the gain

medium, the stability of the DFB resonator in providing feedback could also influence the laser performance in the long term. Especially, HPDLC grating is an all-organic grating, in which the periodic structure may degrade with the elapse of time. The measurements were carried on with a conjugated polymer laser fabricated 10 months ago. The sample was stored in dark under ambient atmosphere, and we measured the threshold of the device once a month. The result of the test is shown in Fig. 8. The variation in laser threshold is within the error of these measurements, demonstrating the stability of HPDLC gratings in providing feedback.

5. Conclusion

In conclusion, we have fabricated and characterized the second-order DFB polymer laser based on a small period HPDLC grating. The separate organic grating on top of the homogeneous conjugated polymer layer serves as natural encapsulation to protect it from oxygen and moisture. The laser shows a vertically emitting laser emission with a threshold of 13.3 µJ/cm² and a bandwidth of 0.6 nm. We explained the dependence of threshold on pumping length, and showed the refractive index modulation afforded by this all organic grating is sufficient for obtaining efficient feedback for lasing output as long as the pumping length is no less than 0.03 cm. Further, the device shows merely degradation in laser performance after 10 months of storage, indicating the reliability of the organic grating as a DFB resonator. We think this "organic" approach for realizing microstructures is extremely compatible with the processing technique of organic semiconductors and is very promising in realizing ultra-low all plastic DFB lasers.

Acknowledgment

The authors would like to thank the financial support from the Natural Science Foundation of China (Grant Nos. 61205021, 11174274, 11174279, 11204299).

Appendix A. Supplementary material

Supplementary data associated with this article can be found, in the online version, at http://dx.doi.org/10.1016/j.orgel.2013.05.025.

References

- D. Moses, High quantum efficiency luminescence from a conducting polymer in solution: a novel polymer laser dye, Appl. Phys. Lett. 60 (1992) 3215–3217.
- [2] M.D. McGehee, A.J. Heeger, Semiconducting (conjugated) polymers as materials for solid-state lasers, Adv. Mater. 12 (2000) 1655–1668.
- [3] I.D.W. Samuel, G.A. Turnbull, Organic semiconductor lasers, Chem. Rev. 107 (2007) 1272–1295.
- [4] C. Gärtner, C. Karnutsch, U. Lemmer, C. Pflumm, The influence of annihilation processes on the threshold current density of organic laser diodes, J. Appl. Phys. 101 (2007) 023107.
- [5] M. Lehnhardt, T. Riedl, T. Weimann, W. Kowalsky, Impact of triplet absorption and triplet-singlet annihilation on the dynamics of optically pumped organic solid-state lasers, Phys. Rev. B 81 (2010) 165206.

- [6] C. Karnutsch, M. Stroisch, M. Punke, U. Lemmer, J. Wang, T. Weimann, Laser diode-pumped organic semiconductor lasers utilizing two-dimensional photonic crystal resonators, IEEE Photonics Technol. Lett. 19 (2007) 741–743.
- [7] Y. Yang, G.A. Turnbull, I.D.W. Samuel, Hybrid optoelectronics: a polymer laser pumped by a nitride light-emitting diode, Appl. Phys. Lett. 92 (2008) 163306.
- [8] G. Heliotis, R. Xia, G.A. Turnbull, P. Andrew, W.L. Barnes, I.D.W. Samuel, D.D.C. Bradley, Emission characteristics and performance comparison of polufluorene lasers with one- and two-dimensional distributed feedback, Adv. Funct. Mater. 14 (2004) 91–97.
- [9] M. Gaal, C. Gadermaier, H. Plank, E. Moderegger, A. Pogantsch, G. Leising, E.J.W. List, Imprinted conjugated polymer laser, Adv. Mater. 15 (2003) 1165–1167.
- [10] V. Navarro-Fuster, I. Vragovic, E.M. Calzado, P.G. Boj, J.A. Quintana, J.M. Villalvilla, A. Retolaza, A. Juarros, D. Otaduy, S. Merino, M.A. Díaz-García, Film thickness and grating depth variation in organic second-order distributed feedback lasers, J. Appl. Phys. 112 (2012) 043104
- [11] G.A. Turnbull, P. Andrew, M.J. Jory, W.L. Barnes, I.D.W. Samuel, Relationship between photonic band structure and emission characteristics of a polymer distributed feedback laser, Phys. Rev. B 64 (2001) 125122.
- [12] C. Karnutsch, C. Pflumm, G. Heliotis, J.C. deMello, D.D.C. Bradley, J. Wang, T. Weimann, V. Haug, C. Gärtner, U. Lemmer, Improved organic semiconductor lasers based on a mixed-order distributed feedback resonator design, Appl. Phys. Lett. 90 (2007) 131104.
- [13] G.A. Turnbull, P. Andrew, W.L. Barnes, I.D.W. Samuel, Operating characteristics of a semiconducting polymer laser pumped by a microchip laser, Appl. Phys. Lett. 82 (2003) 313–315.
- [14] B. Wenger, N. Tétreault, M.E. Welland, R.H. Friend, Mechanically tunable conjugated polymer distributed feedback lasers, Appl. Phys. Lett. 97 (2010) 193303.
- [15] J.R. Lawrence, P. Andrew, W.L. Barnes, M. Buck, G.A. Turnbull, I.D.W. Samuel, Optical properties of a light-emitting polymer directly patterned by soft lithography, Appl. Phys. Lett. 81 (2002) 1955–1957
- [16] J.R. Lawrence, G.A. Turnbull, I.D.W. Samuel, Polymer laser fabricated by a simple micromolding process, Appl. Phys. Lett. 82 (2003) 4023– 4025
- [17] C. Ge, M. Lu, X. Jian, Y. Tan, B.T. Cunningham, Large-area organic distributed feedback laser fabricated by nanoreplica molding and horizontal dipping, Opt. Express 18 (2010) 12980–12991.

- [18] T. Zhai, X. Zhang, Z. Pang, F. Dou, Direct writing of polymer lasers using interference ablation, Adv. Mater. 23 (2011) 1860–1864.
- [19] H.-H. Fang, R. Ding, S.-Y. Lu, J. Yang, X.-L. Zhang, R. Yang, J. Feng, Q.-D. Chen, J.-F. Song, H.-B. Sun, Distributed feedback lasers based on thiophene/phenylene co-oligomer single crystals, Adv. Funct. Mater. 22 (2012) 33–38
- [20] W. Huang, Z. Diao, Y. Liu, Z. Peng, C. Yang, J. Ma, L. Xuan, Distributed feedback polymer laser with an external feedback structure fabricated by holographic polymerization technique, Org. Electron. 13 (2012) 2307–2311.
- [21] W. Huang, Y. Liu, Z. Diao, C. Yang, L. Yao, J. Ma, L. Xuan, Theory and characteristics of holographic polymer dispersed liquid crystal transmission grating with scaffolding morphology, Appl. Opt. 51 (2012) 4013–4020.
- [22] R. Caputo, A.V. Sukhov, N.V. Tabirian, C. Umeton, R.F. Ushakov, Mass transfer processes induced by inhomogeneous photopolymerisation in a multicomponent medium, Chem. Phys. 271 (2001) 323–335.
- [23] R.F. Kazarinov, C.H. Henry, Second-order distributed feedback lasers with mode selection provided by first-order radiation losses, IEEE J. Quantum Electron QE-21 (1985) 144–150.
- [24] M. Salerno, G. Gigli, M. Zavelani-Rossi, S. Perissinotto, G. Lanzani, Effects of morphology and optical contrast in organic distributed feedback lasers, Appl. Phys. Lett. 90 (2007) 111110.
- [25] V.M. Fitio, O.V. Sakhno, T.N. Smirnova, Analysis of the diffraction by the gratings generated in the materials with a nonlinear response, Optik 119 (2008) 236–246.
- [26] H. Kogelnik, C.V. Shank, Coupled-wave theory of distributed feedback lasers, J. Appl. Phys. 43 (1972) 2327–2335.
- [27] M.D. McGehee, R. Gupta, S. Veenstra, E.K. Miller, M.A. Díaz-García, A.J. Heeger, Amplified spontaneous emission from photopumped films of a conjugated polymer, Phys. Rev. B 58 (1998) 7035–7039.
- [28] E.M. Calzado, J.M. Villalvilla, P.G. Boj, J.A. Quintana, V. Navarro-Fuster, A. Retolaza, S. Merino, M.A. Díaz-García, Influence of the excitation area on the thresholds of organic second-order distributed feedback lasers, Appl. Phys. Lett. 101 (2012) 223303.
- [29] J. Herrnsdorf, B. Guilhabert, Y. Chen, A.L. Kanibolotsky, A.R. Mackintosh, R.A. Pethrick, P.J. Skabara, E. Gu, N. Laurand, M.D. Dawson, Flexible blue-emitting encapsulated organic semiconductor DFB laser, Opt. Express 18 (2010) 25535–25545.
- [30] S. Richardson, O.P.M. Gaudin, G.A. Turnbull, I.D.W. Samuel, Improved operational lifetime of semiconducting polymer lasers by encapsulation, Appl. Phys. Lett. 91 (2007) 261104.